

University of Groningen

## Blowfly flight and optic flow I. Thorax kinematics and flight dynamics

Schilstra, C; Van Hateren, JH

*Published in:*  
Journal of Experimental Biology

**IMPORTANT NOTE: You are advised to consult the publisher's version (publisher's PDF) if you wish to cite from it. Please check the document version below.**

*Document Version*  
Publisher's PDF, also known as Version of record

*Publication date:*  
1999

[Link to publication in University of Groningen/UMCG research database](#)

*Citation for published version (APA):*  
Schilstra, C., & Van Hateren, JH. (1999). Blowfly flight and optic flow I. Thorax kinematics and flight dynamics. *Journal of Experimental Biology*, 202(11), 1481-1490.

### Copyright

Other than for strictly personal use, it is not permitted to download or to forward/distribute the text or part of it without the consent of the author(s) and/or copyright holder(s), unless the work is under an open content license (like Creative Commons).

The publication may also be distributed here under the terms of Article 25fa of the Dutch Copyright Act, indicated by the "Taverne" license. More information can be found on the University of Groningen website: <https://www.rug.nl/library/open-access/self-archiving-pure/taverne-amendment>.

### Take-down policy

If you believe that this document breaches copyright please contact us providing details, and we will remove access to the work immediately and investigate your claim.

*Downloaded from the University of Groningen/UMCG research database (Pure): <http://www.rug.nl/research/portal>. For technical reasons the number of authors shown on this cover page is limited to 10 maximum.*

# BLOWFLY FLIGHT AND OPTIC FLOW

## I. THORAX KINEMATICS AND FLIGHT DYNAMICS

C. SCHILSTRA AND J. H. VAN HATEREN\*

*Department of Neurobiophysics, University of Groningen, Nijenborgh 4, NL-9747 AG Groningen, The Netherlands*

\*Author for correspondence (e-mail: hateren@bcn.rug.nl)

*Accepted 4 March; published on WWW 6 May 1999*

### Summary

The motion of the thorax of the blowfly *Calliphora vicina* was measured during cruising flight inside a cage measuring 40 cm×40 cm×40 cm. Sensor coils mounted on the thorax picked up externally generated magnetic fields and yielded measurements of the position and orientation of the thorax with a resolution of 1 ms, 0.3° and 1 mm. Flight velocities inside the cage were up to 1.2 m s<sup>-1</sup>, and accelerations were up to 1 g (≈10 m s<sup>-2</sup>) vertically and 2 g horizontally. During flight, blowflies performed a series of short (approximately 20–30 ms) saccade-like turns at a rate of approximately 10 s<sup>-1</sup>. The saccades consisted of a succession of rotations around all axes, occurring in a fixed order. First, a roll was started. Second, the rolled thorax pitched (pulling the nose up) and yawed, resulting in a turn

relative to the outside world. Finally, the thorax rolled back to a level position. Saccades had yaw amplitudes of up to 90°, but 90% were smaller than 50°. Maximum angular velocities were 2000° s<sup>-1</sup>, and maximum accelerations were 10<sup>5</sup>° s<sup>-2</sup>. The latter correspond to torques consistent with the maximal force (2×10<sup>-3</sup> N) that can be generated by the flight motor as inferred from the maximal linear acceleration. Furthermore, the sequence of energy investment in consecutive rotations around different axes appears to be optimized during a saccade.

Key words: *Calliphora vicina*, saccade, search coil, insect flight, blowfly.

### Introduction

Insect flight is an intriguing phenomenon with regard to the aerodynamics and the control of flight. It has long been a mystery how insects can fly, because the lift forces calculated using classical steady aerodynamics are too small to keep them airborne. Only during the last decades it has become clear that unsteady mechanisms, including vortices produced by wing motion, are needed to explain the production of the necessary lift (e.g. Dickinson and Götz, 1993; Ellington et al., 1996; Liu et al., 1998). Although the basic principles of the aerodynamics of insect flight may now gradually become resolved, the control of flight still remains an intricate matter. The nervous system of Diptera, for example, receives information about flight performance from a rich variety of sensors (such as the compound eyes, ocelli, halteres and wing and neck sensors; for a review, see Hengstenberg, 1992) and generates a diverse output in the form of flight muscle activity (with a range of power and steering muscles). Despite this complexity, considerable progress has been made in elucidating the role of several of these sensory inputs (halteres: Nalbach, 1993; Fayyazuddin and Dickinson, 1996; compound eye: Götz and Wandel, 1984; Wagner, 1986c). Furthermore, much is now known about, for example, flight muscle activity (Heide and Götz, 1996), wing kinematics (Lehmann and Dickinson, 1998), flight forces (Kimmerle et al., 1997; Lehmann and Dickinson,

1998) and the kinematics of flight (Land, 1993; Wagner, 1986b,c). The ultimate goal is to understand how the various sensors and outputs are integrated for performing flight manoeuvres during free flight. Therefore, it is essential to have detailed knowledge of free-flight behaviour.

Many species of houseflies and blowflies exhibit different kinds of flight behaviour, depending on the circumstances. Flight can be divided into two basic categories: chasing flight and cruising flight. During chasing, flight is mainly under the control of the visual system (Land, 1993; Wagner, 1986c; Zeil, 1983; Wehrhahn et al., 1982). The fly continuously tries to adjust its orientation such that the angle between its longitudinal body axis and the target decreases. During cruising flight, flies mostly try to stabilize their body orientation under the control of the visual system and the halteres, while changes in orientation appear to occur in a stepwise manner. This strategy has been measured in the hoverfly *Syrirta pipiens* (Collett, 1980), the housefly *Musca domestica* (Wagner, 1986a) and the blowfly *Calliphora vicina* (while tethered; Land, 1973, 1975). However, the temporal resolution of these measurements was limited (typically 20 ms) and not all degrees of freedom could be measured simultaneously. Clearly, for studying flight control, more detailed measurements of flight dynamics are needed given the agility of flies.

Therefore, we present here detailed measurements on the flight behaviour of almost freely flying *Calliphora vicina*. Furthermore, we investigate the consequences of flight behaviour for the visual system. During the experiments, the visual surroundings were stationary, and the fly performed cruising flight. In this article, we present the results of measurements performed on thorax motion only; in the accompanying article (van Hateren and Schilstra, 1999), head movements are considered. The measurements were performed using a new method that has a high temporal, angular and spatial resolution (Schilstra and van Hateren, 1998a), providing information on the structure of the flight manoeuvres and the forces involved on a millisecond time scale. From the measured kinematics, we can derive properties of the flight motor and gain more insight into the forces and torques during flight. Although the abdomen is probably involved in motion control (Zanker, 1988), we only measured thorax motion because the wings, which provide the flight forces, are directly attached to the thorax. Furthermore, it is the motion of the thorax that has direct consequences for the motion of the head and thus for the visual system.

## Materials and methods

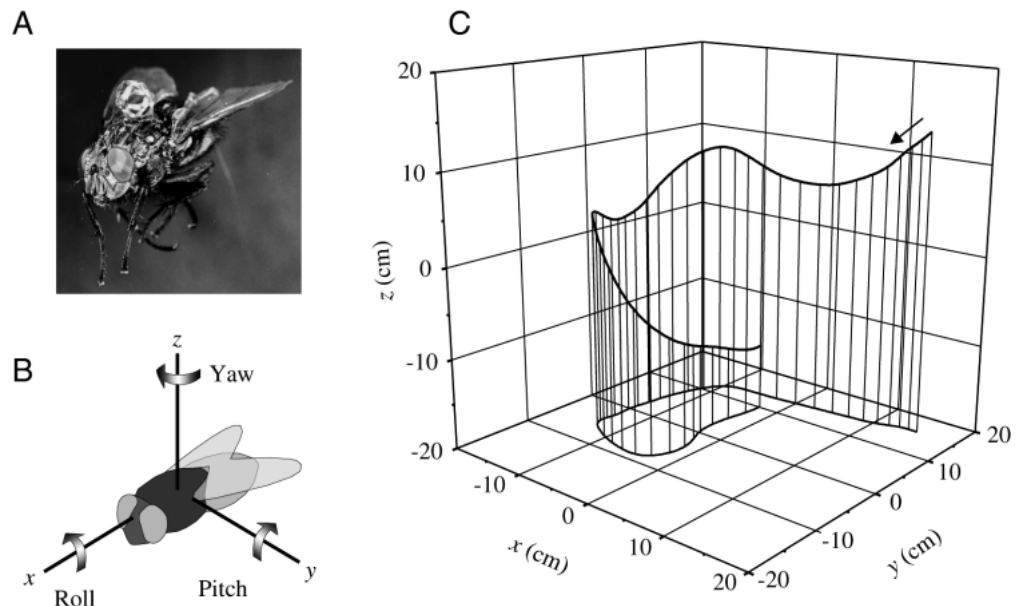
### Position and orientation measurements

We used a modified search coil technique for measuring the position and orientation of the thorax of blowflies flying in a cage measuring 40 cm×40 cm×40 cm. The method is summarized here; for further details, see Schilstra and van Hateren (1998a). Three orthogonal pairs of field coils, surrounding the flight cage, produce magnetic fields oscillating at different frequencies (50, 68 and 86 kHz). Two of these fields are approximately homogeneous, the third has strong

gradients in all directions. The fields induce voltages in a system of three small orthogonal sensor coils attached to the thorax of a blowfly (Fig. 1A). The diameter of each sensor coil is 2 mm, it consists of 80 windings of copper wire (diameter 12  $\mu\text{m}$ ), and the total mass of the three coils is 1.6 mg. The six connecting copper wires run from the coils, *via* the abdomen, to the bottom of the cage. The wires are twisted to prevent unwanted pick-up of magnetic flux. The mass of the cable formed by the twisted wires (i.e. the mass of the part that the fly had to lift) was less than 6 mg during measurements. This mass is small compared with the mass (80–100 mg) of the blowflies used in the experiments. We investigated the possible influence of the weight of the cable on flight performance by performing measurements on blowflies to which a second cable was attached (doubling the weight); subsequently, this cable was removed. We found no difference between the flight statistics (such as histograms of velocities and accelerations) for the two conditions. Finally, we observed that the cable always hung nearly vertically during flight, and conclude that drag on the cable caused by air friction is small compared with the weight of the cable.

The wires from the three sensor coils are connected to nine lock-in amplifiers which separate and measure the signals induced in each of the sensor coils. The orientation of the sensor coil system is the main factor determining the voltages induced by the homogeneous fields. The position of the sensor coil system, in contrast, is the main factor determining the voltages induced by the gradient field. Therefore, with appropriate calibration of sensor coils and magnetic fields, it is possible to reconstruct the position and orientation of the blowfly from the outputs of the lock-in amplifiers. These outputs were sampled at a rate of 1 kHz and stored on hard disk. The reconstruction of position and orientation was

Fig. 1. (A) A blowfly with sensor coils attached to the thorax. The cable running from the coils to the bottom of the cage is just visible hanging down from the abdomen. (B) Definition of yaw, pitch and roll rotations. Arrows define the positive rotation directions used throughout this article. See text for further explanation. (C) Example of a measured flight path with a duration of 2 s. The walls of the flight cage were situated at  $-20$  cm and  $+20$  cm for all axes. The trace starts in the upper right corner, with the arrow showing the direction of flight. A projection onto the horizontal plane is shown on the bottom plane, with vertical lines demarcating periods of 50 ms. The position coordinates were smoothed using a Gaussian function with  $\sigma=10$  ms to reduce noise; this did not noticeably alter the shape of the actual trajectory. A short movie of a reconstructed flight can be found at [http://hlab.phys.rug.nl/demos/flying\\_eye](http://hlab.phys.rug.nl/demos/flying_eye).



performed off-line. The angular accuracy of this method is approximately  $0.3^\circ$ , and the spatial accuracy is approximately 1 mm (Schilstra and van Hateren, 1998a).

#### Preparation and flight recording

Experiments were performed on 1- to 2-week-old female blowflies (*Calliphora vicina* R.-D.) from the offspring ( $F_1$ ) of flies caught in the wild. During preparation, the fly was restrained by a clamp which gently pressed two pads of soft material laterally onto the fly, leaving the dorsal part of the thorax freely accessible. Hairs on the thorax interfering with mounting the coils were cut away. The sensor coil system was glued to the dorsal part of the thorax using a tiny amount of cyanoacrylate adhesive. It was mounted such that the orientation of the three sensor coils was approximately aligned with the body axes of the fly. Deviations from the standard orientation and position of the sensor coil system on the thorax were estimated and corrected for in the reconstruction

program. The position of the fly as presented below is given for a point midway between the points of attachment of the wings. The orientation of the thorax coordinate system is given by a longitudinal axis through this point (parallel to the dorsal surface of the thorax directly above this point) and two orthogonal axes running left-right and vertically. The cable consisting of the six twisted wires coming from the sensor coils was glued either onto the last or onto the second to last segment of the abdomen, leaving a stretch long enough to permit unrestrained movement of the abdomen with respect to the thorax (for a discussion of the role of the abdomen as an air rudder, see Zanker, 1988). During flight, the cable hung down from the tip of the abdomen, leaving the wings and legs of the fly free to move.

The walls of the flight cage were covered with transparencies onto which photographs showing leaves, grass and flowers were printed and which were illuminated from the outside through frosted paper. The ceiling was covered with

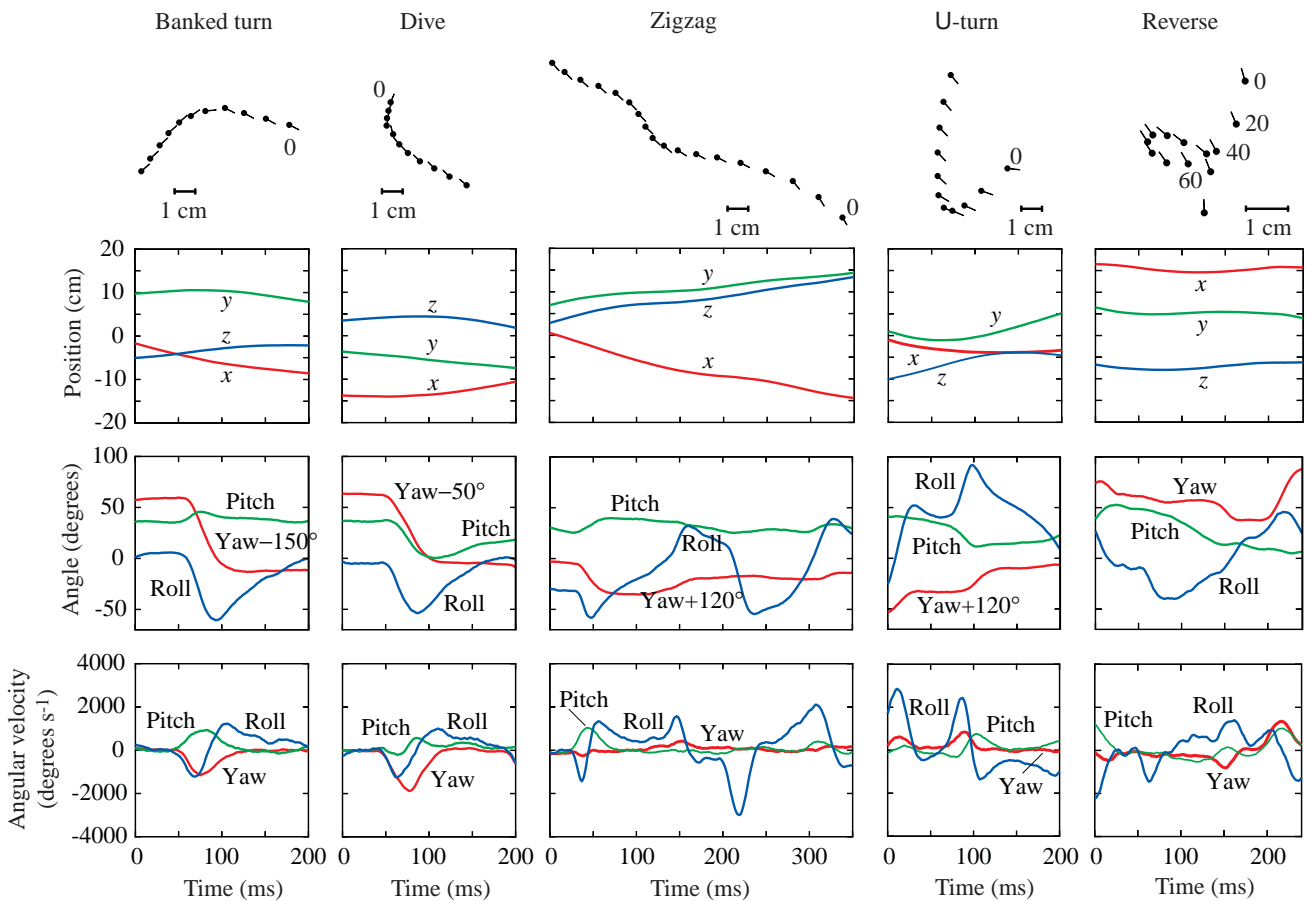


Fig. 2. Five distinct flight manoeuvres. Each column shows, for one particular manoeuvre, the same time track for each of its panels. The first row shows the projection of the flight trajectory on the  $x$ - $y$  plane. The position of the fly is drawn every 20 ms. To reduce noise, the coordinates were smoothed using a Gaussian function with  $\sigma=10$  ms. The orientation of the lines gives the orientation of the longitudinal body axis (yaw), the centre of the lines gives the position of the centre of the thorax (as defined in Materials and methods) and the dots indicate the head. The second row shows the position corresponding to the first row, including the height (position on the  $z$ -axis, drawn at every millisecond). The third row shows the orientational angles of the fly in the laboratory system (see Fig. 1B). For the purposes of presentation, the yaw angle has been shifted vertically in four of the panels. The bottom row shows angular velocities with respect to the thorax coordinate system; it was smoothed using a Gaussian function with  $\sigma=4$  ms, which did not appreciably alter the shape of the actual angular velocity trajectory.

brightly lit frosted paper onto which random lines and dots were drawn. This provided the fly with depth clues, preventing it from accidentally flying into the ceiling. The mean luminance of the walls was  $150 \text{ cd m}^{-2}$  and that of the ceiling was  $800 \text{ cd m}^{-2}$ .

The fly was cooled for 15 min at  $3^\circ \text{C}$  before being released into the flight cage. This prevented it from escaping immediately after release, when the entrance of the cage was still open. After warming up for a couple of minutes, flies typically started to make a series of flights, some very short (less than 0.5 s), most of intermediate length (a couple of seconds) and some lasting up to several tens of seconds. The flights were interspersed by periods of sitting or walking on the walls of the cage. Although an experiment could last up to several hours, the total amount of true flying time was limited to a maximum of 10–20 min. This limitation was caused by the formation of loops in the cable attached to the fly. These loops were formed because flies always produced a net rotation of the cable after performing a large series of rotations in various directions. Care was taken to stop the experiment before the loops in the cable could interfere with normal flight (because of the shortening of the cable and the added weight). For the analysis below, the results of experiments on 10 flies were used; only flights of at least 2 s duration were included, yielding a total flight time of 1781 s.

#### Angular coordinates

A blowfly in flight has six degrees of freedom for its movement: it can translate in three dimensions in space and rotate around three orthogonal axes. The orientation of a body with respect to a reference orientation is often described by three angles in a Fick system:  $\theta$ ,  $\phi$  and  $\psi$  (Haslwanter, 1995). To reach a desired orientation, the body has to be rotated in a fixed sequence around the three body axes, starting from a reference orientation. In a Fick system, the body is first rotated around its  $z$ -axis with angle  $\theta$ , followed by a rotation around its (resulting)  $y$ -axis with angle  $\phi$ , and finally around its (resulting)  $x$ -axis with angle  $\psi$  (Fig. 1B). It is important to note that the axes of rotation are not fixed in space, but rotate with each subsequent rotation (as in a gimbal system). Mathematically, the directions of the three rotations are determined by following the right-hand rule. For all computations, we used this mathematical convention (following Haslwanter, 1995). However, to present the measurements of flight behaviour, it is helpful to use the more common aeronautical description. In aeronautics, the convention is to call  $-\theta$  the yaw angle (positive for turning to the right),  $-\phi$  the pitch angle (positive for pulling the nose up) and  $\psi$  the roll angle (positive for a roll to the right). We use the aeronautical convention, as shown by the arrows in Fig. 1B, throughout this article.

The yaw, pitch and roll angles give a complete description of all possible manoeuvres with respect to the laboratory system. However, the angular velocities and accelerations that are of most importance for flight control (related to the forces produced by the fly) are those defined in the coordinate system

of the fly itself. To appreciate the important difference between angular rotations defined in the laboratory coordinate system and those in the thorax coordinate system, consider the following two examples of hypothetical manoeuvres. In the first example, the thorax system starts with the same orientation as the laboratory system and then yaws  $90^\circ$  around the vertical axis of the laboratory system, which in this case coincides with the fly's vertical axis. In the second example, the fly starts in a  $90^\circ$  rolled orientation and then pitches  $90^\circ$  around its own lateral axis, which in this case coincides with the vertical axis of the laboratory system. In both examples, the fly rotates  $90^\circ$  around the vertical laboratory axis, but the axes around which the fly rotates in its own system are different. This implies that the fly has to use its muscles in a different way to produce different torques, whereas the rotation in the laboratory system appears to be the same.

## Results

Fig. 1C shows an example of 2 s of flight. The fly performs several turns while it descends. The vertical lines drawn at 50 ms intervals indicate the distance travelled and the height of the fly. As illustrated, a typical flight path of *Calliphora vicina* is characterized by smooth curves. These gradual changes in position are almost always caused by abrupt changes in thorax orientation, which change the direction of the force vector generated by the wings (Wagner, 1986a). Unless the change in thorax orientation is quite large, the resulting flight path remains relatively smooth because of the inertia of the fly. Although a large majority of these thorax turns are of one particular type, the so-called banked turn, the blowfly in fact has a rich repertoire of flight manoeuvres available. Before concentrating on the detailed properties of the banked turn, we will first describe examples of several different manoeuvres.

#### Examples of flight manoeuvres

The first column of Fig. 2 gives an example of the most common manoeuvre: the 'banked turn'. It is similar to the way that aeroplanes or helicopters usually turn: by rolling (rotating around a longitudinal axis), the mean force vector generated by the flight motor acquires a sideways component in the laboratory coordinate system, inducing a change of flight course. Assuming that the two force vectors produced by the fly's wings are restricted to lie in vertical planes parallel to the plane defined by the yaw and roll axes of Fig. 1B (Wagner, 1986a; Götz and Wandel, 1984), the only way a blowfly can then produce sideways accelerations is by rolling its body. The graph in the upper row of Fig. 2 is a horizontal projection of the flight path in which the orientation of the lines shows the orientation (yaw) of the thorax at 20 ms intervals. The filled circles symbolize the fly's head. The yaw angle changes in a stepwise manner by approximately  $70^\circ$  in 50 ms, remaining stable before and after this turn. Because of the similarity between this behaviour and that of the human eye when it makes a saccade (a fast gaze shift, see Carpenter, 1988), these

thorax turns are also called thorax saccades (Land, 1973; Wagner, 1986a).

The abrupt change in yaw is also visible in the graph in the third row of Fig. 2, which further indicates that the roll angle is first increased and subsequently decreased after most of the change in yaw has occurred (see also Fig. 3). This decrease continues, at a lower angular velocity, after the actual (yaw) saccade has finished, thus bringing the thorax back into a horizontal orientation. The pitch typically changes only little during a saccade, at least as seen in the coordinates of the laboratory system. A different pattern is seen, however, for coordinates of the system fixed to (and moving along with) the thorax. The graph in the bottom row of Fig. 2 shows the change, per unit of time, in the yaw, pitch and roll of the thorax at a particular time relative to its own coordinate system 1 ms earlier. The resulting angular velocities are those that the thorax generates relative to its own orientation and are thus linked directly to the required torques and to muscle activity. As the graph shows, a banked turn is characterized by a positive pitch velocity in the system of the thorax when the fly has a non-zero roll in the laboratory system. As in the examples discussed in the Materials and methods section, such a pitch movement produces a change in the yaw angle in the laboratory system. Furthermore, the fly yaws in its own system (Fig. 2; bottom row) to prevent the pitch in the laboratory system (Fig. 2; third row) from increasing too much. At the start of the section of a flight shown here, the pitch angle is approximately  $30^\circ$ , a typical value for slow straight flight. It changes slightly during the turn, but is brought back to  $30^\circ$  after the turn.

Although the above example of a banked turn is a typical case, there are in fact many variations possible that yield slightly different outcomes. An example is shown in the second column of Fig. 2, the 'dive'. This manoeuvre differs from the previous one mainly in the values of pitch: here, there is an almost zero net pitch movement in the thorax system (Fig. 2; bottom row), while the other rotational movements remain similar to those of the banked turn. The yaw movement in the thorax system, while the fly is in a rolled orientation, causes a decreasing pitch in the laboratory system. The effect is further enhanced by the yaw velocity, which is higher than in the banked turn. The fly rolls back into a horizontal position after the yaw turn has been completed. In this case, the nearly zero

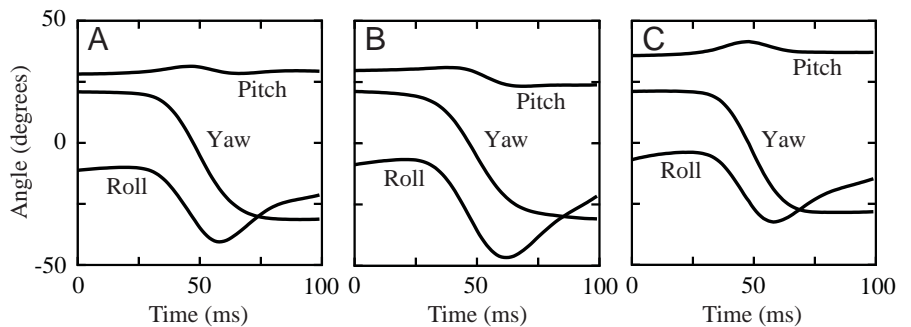
pitch angle is also slowly brought back to a normal value. The sharp initial decrease in the pitch angle results in a transient decrease in the vertical component of the force generated by the flight motor. The subsequent loss of height (hence the name 'dive') can be seen in the plot of the  $z$  coordinate (Fig. 2; second row).

Changes in course can also be made by pure roll movements. This is shown in the manoeuvre 'zigzag' (third column of Fig. 2). It is characterized by a sequence of sideways movements during which the yaw angle changes very little compared with the roll angle. The movement made in the first 100 ms is again a variation on the banked turn, this time without a leftward yaw velocity in the thorax system, which causes the pitch in the laboratory system to increase. During the last 250 ms, the actual zigzag manoeuvre takes place. The large roll angles (Fig. 2; third row) are accomplished by alternating positive and negative roll velocities (Fig. 2; bottom row), while the yaw and pitch velocities in the thorax system remain virtually zero. The force vector therefore acquires a sideways component which alternately points to the left and right of the fly, causing sideways movements.

An almost  $180^\circ$  change in course direction accompanied by a much smaller change in the yaw angle is depicted in the fourth column of Fig. 2 (the 'U-turn'). It contains two saccades, one starting at 0 ms and ending at 30 ms, the second starting at 70 ms and ending at 120 ms. During the second saccade, the fly's longitudinal body axis reaches a nearly perpendicular orientation with respect to the flight direction, while the roll angle reaches a value as high as  $90^\circ$  at 100 ms. This gives the force vector a large component opposing the direction of flight, which subsequently changes the flight direction by nearly  $180^\circ$ . Between 70 and 100 ms, the pitch angle in the laboratory system drops considerably because the fly yaws to the right in its own system (positive yaw velocity) while it has a roll angle between  $45^\circ$  and  $90^\circ$ . At the same time, the yaw angle in the laboratory system changes by  $25^\circ$  because the fly produces a positive pitch velocity in its own system. The second saccade again shows that a positive pitch velocity changes the yaw angle in the laboratory system when the fly is rolled.

As shown in the column termed 'reverse', blowflies are able to fly backwards, although only for a very short time. This manoeuvre is characterized by a very large pitch angle ( $>50^\circ$ ),

Fig. 3. Averages for three different flies of saccades with a yaw change (in the laboratory system) of  $40\text{--}60^\circ$  to the left; averages are for 356, 138 and 119 saccades in A, B and C, respectively. The curves were obtained by detecting saccades through maxima of the total angular velocity in the thorax coordinate system (after low-pass filtering using a Gaussian function with  $\sigma=5$  ms to reduce noise). The detected peak was set at 50 ms, and the 100 ms yaw, pitch and roll angles surrounding the detection point were averaged.



Offsets of the yaw traces are arbitrary, and these traces were shifted to fit the scale of the graphs.

which gives the force vector a component pushing the fly backwards rather than forwards. The sideways motion is controlled by large rolling movements. The manoeuvre ends with a banked turn. 'Reverse' manoeuvres are rare and are only seen in the vicinity of a wall of the flight cage. Like the U-turn, part of their function may be to act as a kind of emergency brake.

### Structure of saccades

The banked turn is the most common saccadic manoeuvre blowflies perform. Most flights consist of a long series of such turns (see Fig. 3 in van Hateren and Schilstra, 1999). The structure of these saccades is not only similar within a fly, but also among flies. Fig. 3 shows, for three different flies, the averaged angles for saccades with a yaw change between  $40^\circ$  and  $60^\circ$ . As can be seen, the time courses of the saccades are quite similar: the traces of the angles show the same overall structure, the timing of the changes in the angles is the same and the saccades have the same duration.

Because the saccades measured in different flies are similar, the analysis below will be performed on the pooled measurements from 10 different blowflies. Fig. 4 shows averaged values for saccades with a yaw change of  $10\text{--}20^\circ$  (left column),  $30\text{--}40^\circ$  (middle column) and  $60\text{--}90^\circ$  (right

column). The graphs show that, for larger yaw changes, the change in roll angle is also larger. Because of the roll, the force vector acquires a horizontal component, which produces the sideways acceleration that results in a change of flight course. Simultaneously, the fly increases both the yaw and pitch velocities in its own coordinate system (second row), together producing the increased yaw in the laboratory system. The roll angle and angular velocity are not zero at the onset of an average saccade, although one might expect that the contributions from previous leftward and rightward saccades should approximately cancel each other out. The reason for this apparent discrepancy is that a saccade with a particular yaw direction is more likely to be preceded by a saccade in the same yaw direction than in the opposite direction. Finally, the bottom row in Fig. 4 shows the angular accelerations in the thorax coordinate system, from which the torques generated by the flight motor can be obtained (see Discussion).

### Saccade statistics

Saccades with yaw sizes as large as  $90^\circ$  occur occasionally, but most saccades are much smaller (Fig. 5A). Approximately 90% of the saccades were smaller than  $50^\circ$ . The number of  $0\text{--}10^\circ$  saccades is underestimated in Fig. 5A because measurement noise prevents reliable discrimination of the

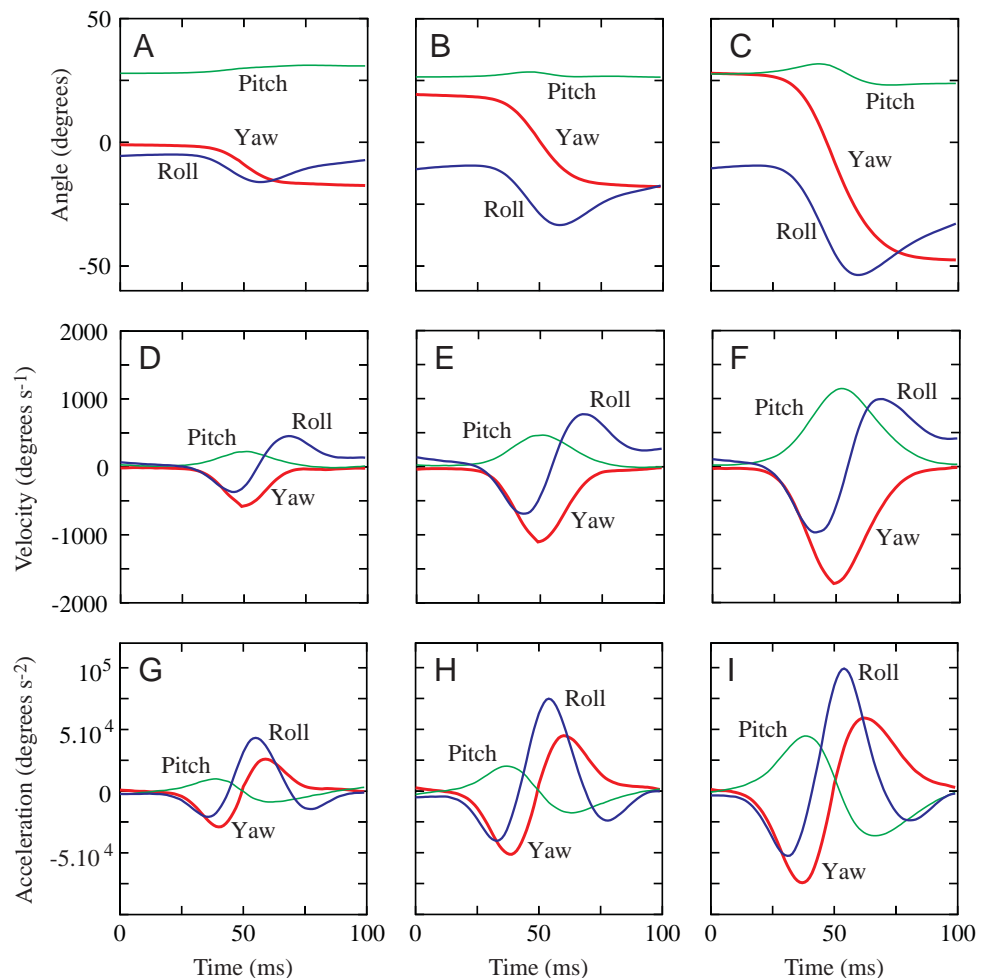
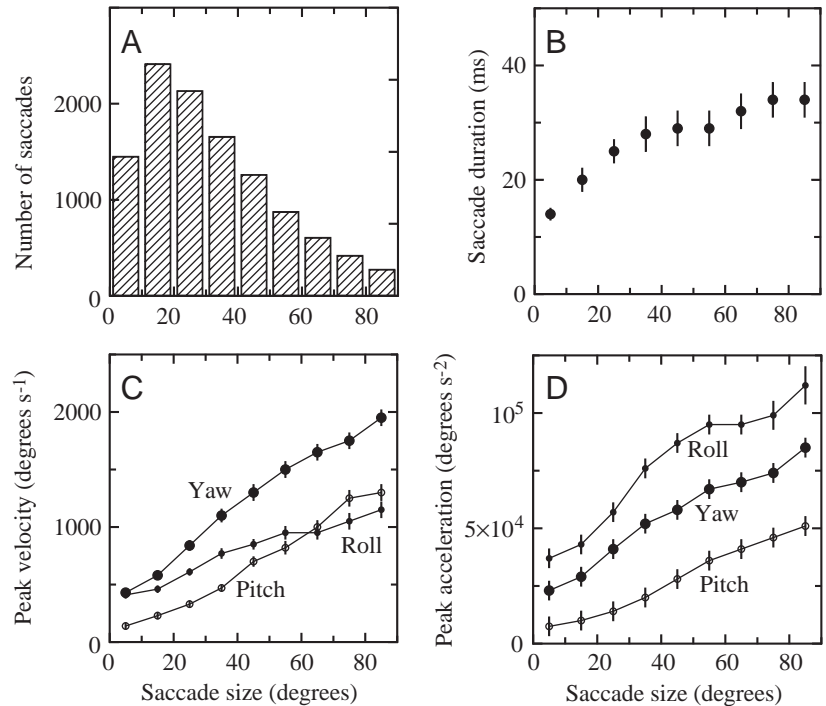


Fig. 4. Averages of saccades from 10 flies showing a yaw change (in the laboratory system) to the left, with a magnitude of  $10\text{--}20^\circ$  (1217 saccades; A,D,G),  $30\text{--}40^\circ$  (946 saccades; B,E,H) and  $60\text{--}90^\circ$  (677 saccades; C,F,I). Saccades were detected as in Fig. 3. (A–C) Yaw, roll and pitch angles in the laboratory system. The yaw trace was shifted to fit the vertical scale. (D–F) Angular velocities in the thorax system, smoothed using a Gaussian function with  $\sigma=2$  ms. (G–I) Angular accelerations in the thorax system, smoothed using a Gaussian function with  $\sigma=5$  ms.

Fig. 5. Saccade statistics as measured in 10 flies. (A) The occurrence of saccades as a function of saccade size, defined as the total yaw change in the laboratory system. Saccades were detected as in Fig. 3. (B) Saccade duration as a function of saccade size. The duration is defined as the rise time (from 10% to 90% amplitude) of the yaw change in the laboratory system. (C) Peak angular velocities (in the thorax coordinate system) during saccades as a function of saccade size. (D) Peak angular accelerations (in the thorax coordinate system) during saccades as a function of saccade size. For the sake of clarity, data points in C and D are connected by lines. Smoothing for C and D was as in Fig. 4. Values for B–D are means  $\pm$  s.d.



smallest saccades. Saccade duration, defined here as the time between reaching 10% and 90% of the yaw change in the laboratory coordinate system, does not depend very strongly on saccade size (Fig. 5B). Since 90% of the saccades were smaller than  $50^\circ$ , it follows that 90% of the saccades have a duration of approximately 20–30 ms (3–4 wingbeat cycles). The saccade duration does not increase strongly because peak angular velocities increase roughly linearly as a function of saccade size (Fig. 5C). Note that, for increasing roll, the relative contribution of the pitch movement increases, as expected. Also, the peak angular accelerations increase significantly with saccade size (Fig. 5D).

#### Velocities and accelerations

Fig. 6 shows the distributions of angular velocities and accelerations, in the thorax coordinate system, for the total flight time. Maximum angular velocities are of the order of  $2000^\circ\text{s}^{-1}$ . The velocity distributions of the yaw and roll are symmetrical, as expected, but the pitch velocity distribution has a clearly asymmetrical shape. This asymmetry is caused by the positive pitch movement that the fly makes (in the thorax coordinate system) during all saccades, irrespective of turning direction. The yaw velocity distribution has a sharp peak and long tails. These arise from the yaw movements between saccades and during saccades, respectively (Schilstra and van Hateren, 1998b; van Hateren and Schilstra, 1999). Angular accelerations (Fig. 6B) reach maximum values of approximately  $10^5^\circ\text{s}^{-2}$ , which are indicative of the maximum torques that can be developed by the flight motor (see Discussion).

The (linear) velocity and acceleration of a fly can be separated into  $x$ ,  $y$  and  $z$  components. In Fig. 7, the  $x$  and  $y$

components of velocity and acceleration are combined into horizontal velocity and acceleration, since all aspects of flight are identical for flying in the  $x$  and  $y$  directions. Fig. 7A shows that horizontal velocities of up to  $1.2\text{ m s}^{-1}$  are reached, approximately twice as high as the mean horizontal velocity. Vertical velocities reach approximately  $0.8\text{ m s}^{-1}$ . Note that the distribution of vertical velocities is virtually symmetrical around zero, despite the asymmetry in the gravitational force. Accelerations in the horizontal plane (Fig. 7B) can be as large as  $2g$  ( $20\text{ m s}^{-2}$ ), apparently reached when the force vector is pointing approximately horizontally (such as during a U-turn). The force associated with this acceleration ( $2 \times 10^{-3}\text{ N}$ , assuming a fly mass of  $100\text{ mg}$ ) is, therefore, the largest linear

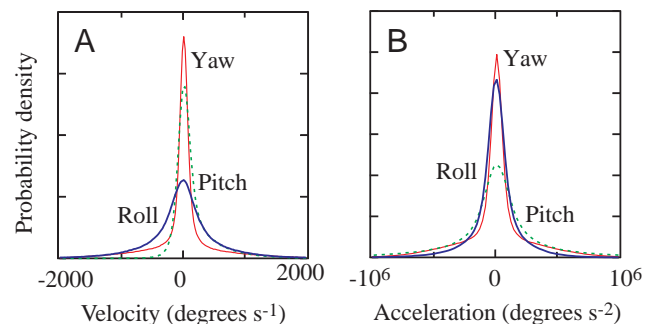


Fig. 6. Probability densities of angular velocities (A) and accelerations (B) as measured in the thorax coordinate system for 1781 s of flight by 10 flies. Probability densities were calculated for angular velocities and accelerations filtered using Gaussian functions with  $\sigma=2\text{ ms}$  and  $\sigma=5\text{ ms}$ , respectively, to reduce noise. Full scale,  $4 \times 10^{-3}\text{ degree}^{-1}\text{ s}$  for A and  $6 \times 10^{-5}\text{ degree}^{-1}\text{ s}^2$  for B. Roll, blue; yaw, red; pitch, green.



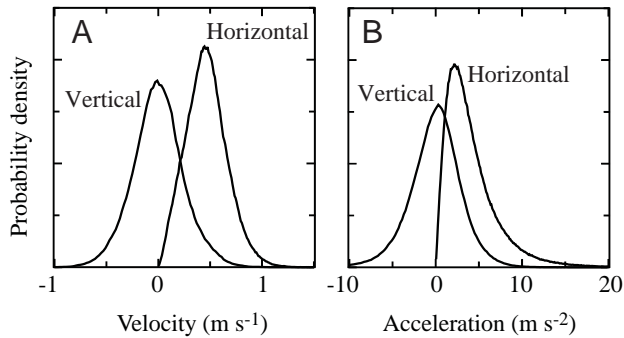


Fig. 7. Probability densities of linear velocities and accelerations as measured in the laboratory coordinate system for 1781 s of flight by 10 flies. Probability densities were calculated for velocities and accelerations filtered using Gaussian functions with  $\sigma=5$  ms and  $\sigma=10$  ms, respectively, to reduce noise. Full scale,  $2.5 \text{ m}^{-1} \text{ s}$  for A and  $0.25 \text{ m}^{-1} \text{ s}^2$  for B.

force normally produced by blowflies. In the vertical direction, the accelerations are mostly smaller, up to  $1g$ . This smaller range of vertical acceleration is consistent with the assumption that  $2g$  is the maximum acceleration that is generated. For upward acceleration,  $1g$  is used to overcome gravity, leaving another  $1g$  for accelerated flight. Downward acceleration is apparently mainly limited by gravity ( $-1g$ ).

### Discussion

Cruising flight of the blowfly *Calliphora vicina* has similar saccadic characteristics to those measured previously in the housefly *Musca domestica* (Wagner, 1986a). At regular intervals, the orientation of the fly changes abruptly at high angular velocity, while the orientation of the fly is relatively constant between these changes (Schilstra and van Hateren, 1998b; van Hateren and Schilstra, 1999). Saccadic behaviour has been demonstrated previously in tethered blowflies which were able to rotate around their vertical axis (Land, 1973, 1975), but this was later suspected of being an artefact of the tether mass added to the system (Geiger and Poggio, 1977). The experiments presented here clearly confirm that cruising blowflies do indeed show saccadic behaviour. The structure of the average saccade is very stereotyped, largely independent of its size and very similar among flies. However, from the manoeuvres described in the present study, it is clear that flies are able to rotate independently around each of their three body axes (see also Wagner, 1986a). This allows the structure of individual saccades to be precisely adjusted, depending both on the orientation of the fly before the saccade and the intended orientation and course after the saccade.

The main limitation of the present experiments is the size of the flight cage. In general, a smaller flight volume lowers the mean flight velocity (hawkmoth; Stevenson et al., 1995). A lowering of the mean and peak velocities is to be expected because, at higher speeds, collisions with the walls will be difficult to avoid given the inertia of the fly and its minimum reaction time. The maximum speeds we measured,

approximately  $1.2 \text{ m s}^{-1}$ , are indeed appreciably smaller than the speeds reported for blowflies flying in a wind tunnel (approximately  $2\text{--}3 \text{ m s}^{-1}$ ; Nachtigall and Roth, 1983). Furthermore, it is possible that the fast succession of saccades we observed (on average at approximately  $10 \text{ s}^{-1}$ ) was caused by the continuous vicinity of the walls. Nevertheless, in more natural circumstances, blowflies also often cruise close to or amidst objects, and the further influence of a restricted flight volume on their basic flight performance may be quite limited (Wagner, 1986a). In principle, the method used here allows for a substantial increase in the measuring volume, without sacrificing resolution, by further increasing the size of the field coils and the strengths of the magnetic fields.

Saccadic behaviour of the thorax has several advantages for the visual system of the fly. First, the head performs saccadic movements in synchrony with the saccadic movements of the thorax (for a review, see Hengstenberg, 1992), thus reaching a high angular velocity in the laboratory system (Schilstra and van Hateren, 1998b; van Hateren and Schilstra, 1999). This high angular velocity keeps the head saccade very short and thus minimizes the period during which angular motion blurs vision. Second, if thorax saccades did not occur, the fly would necessarily have to rotate in a more gradual way. To prevent continuous motion blur caused by this rotation, the head would still have to make saccadic movements. Since the freedom of movement of the head in the yaw direction is limited to approximately  $10^\circ$ , this implies that the head would have to make very frequent saccadic movements. As a result, the proportion of time with a stabilized gaze would be smaller than it actually is with the occurrence of thorax saccades.

A fly produces more modest angular accelerations during small saccades than during large saccades. Therefore, small saccades take longer than apparently necessary. There may be several reasons for this. First, the angular speed may be constrained by the energy investment required. All the rotational energy a fly puts into a saccade, required for both acceleration and deceleration, is lost. This energy expenditure will be approximately proportional to the square of the maximum angular velocity reached during a saccade (neglecting friction). Thus, from an energetic point of view, it is best to rotate as slowly as possible. The limited angular speed of the smaller (most common) saccades can then be seen as a trade-off between minimization of the saccade duration (and thus of the blur period) and minimization of the energy required to perform the rotations. Second, the angular velocity during small saccades may be limited by the physiology of muscular control. The wingbeat amplitude is one of the factors determining the force produced by a wing (*Drosophila* spp.; Lehmann and Dickinson, 1998). Both in *Drosophila melanogaster* (Heide and Götz, 1996) and in *Calliphora vicina* (Tu and Dickinson, 1996), the steering muscles b1 and b2 control most of the modulation of wingbeat amplitude. In *Calliphora vicina*, it takes several wingbeat cycles to produce large changes in wingbeat amplitude (Tu and Dickinson, 1996). Large angular accelerations can therefore only be reached after several wing

beats. Since the wingbeat duration in *Calliphora vicina* is approximately 7 ms, it may take up to a few tens of milliseconds to reach the highest acceleration, in agreement with the time course of the angular accelerations shown in Fig. 4. For small and short saccades, there may simply not be enough time to build up the high velocities and accelerations that occur during larger and longer saccades.

The high temporal and angular resolution of the measurements presented here enables a more detailed analysis of the structure of saccades than could be performed using earlier measurements, where saccades could only be seen as sharp peaks in the angular velocity (Wagner, 1986a). On the scale of milliseconds, we can see that the maxima in the yaw and pitch velocity nearly coincide at the moment when the roll velocity is close to zero (Fig. 4D–F). Angular accelerations (Fig. 4G–I) are directly related to the torques generated (torque = inertial momentum  $\times$  angular acceleration). We will assume that the forces generating these torques are a (possibly nonlinear, but at least monotonic) function of the energy consumption of the muscles involved: greater acceleration implies a greater force, which implies a greater energy consumption. Then, we can infer from Fig. 4 the ordered sequence of energy investment during a saccade. This is especially illuminating for large, energetically costly, saccades as in Fig. 4I: acceleration extremes are reached first by the roll, second by the yaw and pitch (at close to a zero value for the roll acceleration), third by the roll again (at close to a zero value for the yaw and pitch accelerations), fourth by the yaw and pitch again (at close to a zero value for the roll acceleration) and, finally by the roll again (with decreasing yaw and pitch accelerations). Apparently, the serial investment of energy (force) makes efficient use of the available resources, whilst going through the correct series of movements to bring about the saccade. Clearly, the description given above is only a qualitative preliminary scheme: for a full analysis of the energy balance, a more detailed model of the muscular energy requirements and an analysis of the force required by the (linear) acceleration during a turn are required.

Finally, it appears that the angular accelerations achieved by the thorax are close to the maximum possible, as suggested by a consideration of the forces, masses and moments of inertia involved. The maximum force generated by the wings, in excess of the force necessary to remain airborne, can be estimated from the linear acceleration, ignoring friction. The maximum acceleration was approximately  $2g$  (Fig. 7), which yields a force of  $2 \times 10^{-3} \text{ N}$  (taking 100 mg as a typical mass of a blowfly). The yaw and roll torque a fly can produce depend on the effective point of application of the force on a wing, in the radial direction. For *Calliphora vicina*, the distance from the wingbase to this point is approximately half the length of the wing, i.e. 5 mm (Ennos, 1989), which implies a distance of approximately 7 mm from the fly's centre of mass. Assuming that, during saccades, approximately half the available maximal force of  $2 \times 10^{-3} \text{ N}$  is used for keeping the fly airborne (just cancelling the

gravitational force), and half is available for, and equally divided between, linear acceleration, yaw, pitch and roll, the torque generated in the yaw direction is approximately  $7 \times 10^{-3} \times 2.5 \times 10^{-4} \approx 1.8 \times 10^{-6} \text{ N m}$ . The inertial momentum of the fly in the yaw direction ( $8.8 \times 10^{-10} \pm 1.4 \times 10^{-10} \text{ kg m}^2$ , means  $\pm$  s.d.,  $N=3$ , measured with a torsion pendulum) then gives a maximum angular acceleration of  $2 \times 10^3 \text{ rad s}^{-2} \approx 1.2 \times 10^5 \text{ }^\circ \text{ s}^{-2}$ . This is of the same order of magnitude as the maximum yaw acceleration measured during saccades (approximately  $10^5 \text{ }^\circ \text{ s}^{-2}$ ; Fig. 6). The order of magnitude is also approximately right for the roll acceleration (inertial momentum  $3.4 \times 10^{-10} \pm 0.4 \times 10^{-10} \text{ kg m}^2$ ) and the pitch acceleration (inertial momentum  $7.5 \times 10^{-10} \pm 1.5 \times 10^{-10} \text{ kg m}^2$ ; means  $\pm$  s.d.,  $N=3$ ). For the pitch, the torque is most likely brought about by a forward shift of a few millimetres in the force vector, shifting away from the fly's centre of mass (Zanker, 1988).

The authors wish to thank Lieke Poot and Esther Wiersinga-Post for comments. This research was supported by the Netherlands Organization for Scientific Research (NWO) through the Research Council for Earth and Lifesciences (ALW).

## References

- Carpenter, R. H. S.** (1988). *Movements of the Eyes*. London: Pion.
- Collett, T. S.** (1980). Some operating rules for the optomotor system of a hoverfly during voluntary flight. *J. Comp. Physiol.* **138**, 271–282.
- Dickinson, M. H. and Götz, K. G.** (1993). Unsteady aerodynamic performance of model wings at low Reynolds numbers. *J. Exp. Biol.* **174**, 45–64.
- Ellington, C. P., Van Den Berg, C., Willmott, A. P. and Thomas, A. L. R.** (1996). Leading-edge vortices in insect flight. *Nature* **384**, 626–630.
- Ennos, A. R.** (1989). The kinematics and aerodynamics of the free flight of some Diptera. *J. Exp. Biol.* **142**, 49–85.
- Fayyazuddin, A. and Dickinson, M. H.** (1996). Haltere afferents provide direct, electrotonic input to a steering motor neuron in the blowfly, *Calliphora*. *J. Neurosci.* **16**, 5225–5232.
- Geiger, G. and Poggio, T.** (1977). On head and body movements of flying flies. *Biol. Cybernetics* **25**, 177–180.
- Götz, K. G. and Wandel, U.** (1984). Optomotor control of force of flight in *Drosophila* and *Musca*. II. Covariance of lift and thrust in still air. *Biol. Cybernetics* **51**, 135–139.
- Haslwanter, T.** (1995). Mathematics of three-dimensional eye rotations. *Vision Res.* **35**, 1727–1739.
- Heide, G. and Götz, K. G.** (1996). Optomotor control of course and altitude in *Drosophila melanogaster* is correlated with distinct activities of at least three pairs of flight steering muscles. *J. Exp. Biol.* **199**, 1711–1726.
- Hengstenberg, R.** (1992). Stabilizing head/eye movements in the blowfly *Calliphora erythrocephala*. In *The Head-Neck Sensory Motor System* (ed. A. Berthoz, W. Graf and P. P. Vidal), pp. 49–55. Oxford: Oxford University Press.
- Kimmerle, B., Warzecha, A. K. and Egelhaaf, M.** (1997). Object detection in the fly during simulated translatory flight. *J. Comp. Physiol. A* **181**, 247–255.

- Land, M. F.** (1973). Head movements of flies during visually guided flight. *Nature* **243**, 299–300.
- Land, M. F.** (1975). Head movements and fly vision. In *The Compound Eye and Vision of Insects* (ed. G. A. Horridge), pp. 469–489. Oxford: Clarendon Press.
- Land, M. F.** (1993). The visual control of courtship behaviour in the fly *Poecilobothrus nobilitatus*. *J. Comp. Physiol. A* **173**, 595–603.
- Lehmann, F.-O. and Dickinson, M. H.** (1998). The control of wing kinematics and flight forces in fruit flies (*Drosophila* spp.). *J. Exp. Biol.* **201**, 385–401.
- Liu, H., Ellington, C. P., Kawachi, K., Van Den Berg, C. and Willmott, A. P.** (1998). A computational fluid dynamic study of hawkmoth hovering. *J. Exp. Biol.* **201**, 461–477.
- Nachtigall, W. and Roth, W.** (1983). Correlations between stationary measurable parameters of wing movement and aerodynamic force production in the blowfly (*Calliphora vicina* R.-D.). *J. Comp. Physiol.* **150**, 251–260.
- Nalbach, G.** (1993). The halteres of the blowfly *Calliphora*. I. Kinematics and dynamics. *J. Comp. Physiol. A* **173**, 293–300.
- Schilstra, C. and van Hateren, J. H.** (1998a). Using miniature sensor coils for simultaneous measurement of orientation and position of small, fast-moving animals. *J. Neurosci. Meth.* **83**, 125–131.
- Schilstra, C. and van Hateren, J. H.** (1998b). Stabilizing gaze in flying blowflies. *Nature* **395**, 654.
- Stevenson, R. D., Corbo, K., Baca, L. B. and Quang, D. L.** (1995). Cage size and flight speed of the tobacco hawkmoth *Manduca sexta*. *J. Exp. Biol.* **198**, 1665–1672.
- Tu, M. S. and Dickinson, M. H.** (1996). The control of wing kinematics by two steering muscles of the blowfly (*Calliphora vicina*). *J. Comp. Physiol. A* **178**, 813–830.
- van Hateren, J. H. and Schilstra, C.** (1999). Blowfly flight and optic flow. II. Head movements during flight. *J. Exp. Biol.* **202**, 1491–1500.
- Wagner, H.** (1986a). Flight performance and visual control of flight of the free-flying housefly (*Musca domestica* L.). I. Organization of the flight motor. *Phil. Trans. R. Soc. Lond. B* **312**, 527–551.
- Wagner, H.** (1986b). Flight performance and visual control of flight of the free-flying housefly (*Musca domestica* L.). II. Pursuit of targets. *Phil. Trans. R. Soc. Lond. B* **312**, 553–579.
- Wagner, H.** (1986c). Flight performance and visual control of flight of the free-flying housefly (*Musca domestica* L.). III. Interactions between angular movement induced by wide- and smallfield stimuli. *Phil. Trans. R. Soc. Lond. B* **312**, 581–595.
- Wehrhahn, C., Poggio, T. and Bülthoff, H.** (1982). Tracking and chasing in houseflies (*Musca*). *Biol. Cybernetics* **45**, 123–130.
- Zanker, J. M.** (1988). How does lateral abdomen deflection contribute to flight control of *Drosophila melanogaster*? *J. Comp. Physiol. A* **162**, 581–588.
- Zeil, J.** (1983). Sexual dimorphism in the visual system of flies: the free flight behaviour of male Bibionidae (Diptera). *J. Comp. Physiol.* **150**, 395–412.